Supplement of Atmos. Chem. Phys., 22, 2467–2486, 2022
https://doi.org/10.5194/acp-22-2467-2022-supplement

Supplement of

Free amino acid quantification in cloud water at the Puy de Dôme station (France)

Pascal Renard et al.

Correspondence to: Laurent Deguillaume (laurent.deguillaume@uca.fr) and Anne-Marie Delort (a-marie.delort@uca.fr)

Table S1. Characteristics and Concentrations of AAs for each cloud samples expressed in various units and cloud bio-physico-chemical characterization.

	Sampling characteristics			
Label (dd-mm-yy)	**Sampling date**	**Sampling Start**	**Sampling end**	**Category Renard et al. (2020)**
22-Mar-14	March 22, 2014	07:35	11:00	Marine
3-May-18	May 3, 2018	09:30	14:00	Marine
13-Jun-18	June 13, 2018	10:30	12:30	Marine
24-Aug-18	August 24, 2018	10:50	15:15	Marine
24-Sep-18	September 24, 2018	08:30	16:00	Marine
1-Oct-18	October 1, 2018	11:00	12:45	Marine
8-Oct-18	October 8, 2018	13:15	16:45	Marine
25-Sep-19	September 25, 2019	08:45	12:38	Marine
2-Oct-19	October 2, 2019	14:35	16:45	Marine
22am-Oct-19	October 22, 2019	10:10	13:37	Marine
22pm-Oct-19	October 22, 2019	13:40	16:30	Marine
11-Mar-20	March 11, 2020	08:40	13:40	Marine
17-Jul-20	July 17, 2020	11:36	14:40	Continental

Table S1. Continued.

	Amino acids (µg L^{-1}) diluted (9:1)*																	
Label (dd-mm-yy)	***Ala***	***Arg***	***Asn***	***Asp***	***Gln***	***Glu***	***Gly***	***His***	***Leu / I***	***Lys***	***Met***	***Phe***	***Pro***	***Ser***	***Thr***	***Trp***	***Tyr***	***SUM***
22-Mar-14	17	8	< 4	12	< 4	32	8	12	26	16	4	1	8	22	11	4	7	**188**
3-May-18	19	< 4	2	11	1	6	16	3	10	0	1	5	18	34	13	< 1	5	**144**
13-Jun-18	8	< 7	102	< 5	< 5	5	10	< 6	12	< 6	< 6	< 4	10	8	2	< 5	< 5	**157**
24-Aug-18	26	5	131	15	15	17	21	6	17	2	< 4	11	15	33	28	4	5	**351**
24-Sep-18	11	4	11	4	1	7	14	5	7	3	< 1	3	8	17	21	1	2	**119**
1-Oct-18	69	< 6	31	45	3	22	42	22	41	9	< 1	10	30	157	42	2	21	**546**
8-Oct-18	27	< 6	2	14	< 2	8	18	3	22	< 3	< 1	5	14	36	15	1	5	**170**
25-Sep-19	ND	8	21	ND	6	10	87	ND	ND	8	< 4	18	ND	155	25	5	ND	**343**
2-Oct-19	ND	< 4	67	65	2	22	121	26	68	19	< 1	20	ND	282	49	1	27	**769**
22am-Oct-19	ND	< 4	2	22	< 2	10	48	9	22	6	< 1	6	ND	78	18	0	7	**228**
22pm-Oct-19	ND	2	1	6	< 2	3	57	3	17	< 2	0	4	ND	42	8	4	< 3	**147**
11-Mar-20	54	< 3	2	< 1	< 1	< 2	33	< 4	16	< 2	< 2	9	ND	< 3	3	< 1	2	**119**
17-Jul-20	ND	< 2	4	< 2	6	8	72	< 2	19	2	< 1	10	9	22	9	< 2	8	**169**

*: See Figure S3
ND: Not determined
Concentrations lower than their standard deviation are preceded by the sign "<" (Standard deviation ≈ Limit of Quantification, see Figure S3, Table S3 and Section 3.1).

Table S1. Continued.

	Amino acids (nM)																	
Label (dd-mm-yy)	***Ala***	***Arg***	***Asn***	***Asp***	***Gln***	***Glu***	***Gly***	***His***	***Leu / I***	***Lys***	***Met***	***Phe***	***Pro***	***Ser***	***Thr***	***Trp***	***Tyr***	***SUM***
22-Mar-14	212	51	< 34	100	< 30	243	118	86	220	122	30	7	77	233	103	22	43	**1666**
3-May-18	237	< 26	17	92	8	46	237	21	85	0	7	34	174	359	121	< 5	31	**1468**
13-Jun-18	100	< 45	858	< 42	< 38	38	148	< 43	102	< 46	< 45	< 27	97	85	19	< 27	< 31	**1445**
24-Aug-18	324	32	1102	125	113	129	311	43	144	15	< 30	74	145	349	261	22	31	**3220**
24-Sep-18	137	26	93	33	8	53	207	36	59	23	< 7	20	77	180	196	5	12	**1165**
1-Oct-18	861	< 38	261	376	23	167	622	158	347	68	< 7	67	290	1660	392	11	129	**5430**
8-Oct-18	337	< 38	17	117	< 15	61	266	21	186	< 23	< 7	34	135	381	140	5	31	**1731**
25-Sep-19	ND	51	177	ND	45	76	1288	ND	ND	61	< 30	121	ND	1639	233	27	ND	**3718**
2-Oct-19	ND	< 26	563	543	15	167	1791	186	576	144	< 7	135	ND	2981	457	5	166	**7730**
22am-Oct-19	ND	< 26	17	184	< 15	76	710	64	186	46	< 7	40	ND	825	168	0	43	**2359**
22pm-Oct-19	ND	13	8	50	< 15	23	844	21	144	< 15	0	27	ND	444	75	22	< 18	**1671**
11-Mar-20	673	< 19	17	< 8	< 8	< 15	488	< 29	136	< 15	< 15	61	ND	< 32	28	< 5	12	**1415**
17-Jul-20	ND	< 13	34	< 17	45	61	1066	< 14	161	15	< 7	67	87	233	84	< 11	49	**1901**

ND: Not determined
Concentrations lower than their standard deviation are preceded by the sign "<" (Standard deviation ≈ Limit of Quantification, see Figure S3, Table S3 and Section 3.1).

Table S1. Continued.

	Amino acids (ng m^{-3})*																	
Label (dd-mm-yy)	***Ala***	***Arg***	***Asn***	***Asp***	***Gln***	***Glu***	***Gly***	***His***	***Leu / I***	***Lys***	***Met***	***Phe***	***Pro***	***Ser***	***Thr***	***Trp***	***Tyr***	***SUM***
22-Mar-14	5	3	< 1	4	< 1	10	3	4	8	5	1	0	3	7	3	1	2	60
3-May-18	6	< 1	1	3	0	2	5	1	3	0	0	2	6	11	4	< 0	2	46
13-Jun-18	3	< 2	32	< 2	< 2	2	3	< 2	4	< 2	< 2	< 1	3	3	1	< 2	< 2	50
24-Aug-18	8	2	41	5	5	5	7	2	5	1	< 1	3	5	10	9	1	2	111
24-Sep-18	3	1	3	1	0	2	4	2	2	1	< 0	1	3	5	7	0	1	38
1-Oct-18	22	< 2	10	14	1	7	13	7	13	3	< 0	3	10	50	13	1	7	173
8-Oct-18	9	< 2	1	4	< 1	3	6	1	7	< 1	< 0	2	4	11	5	0	2	54
25-Sep-19	ND	3	7	ND	2	3	28	ND	ND	3	< 1	6	ND	49	8	2	ND	109
2-Oct-19	ND	< 1	21	21	1	7	38	8	22	6	< 0	6	ND	89	16	0	9	244
22am-Oct-19	ND	< 1	1	7	< 1	3	15	3	7	2	< 0	2	ND	25	6	0	2	72
22pm-Oct-19	ND	1	0	2	< 1	1	18	1	5	< 1	0	1	ND	13	3	1	< 1	47
11-Mar-20	17	< 1	1	< 0	< 0	< 1	10	< 1	5	< 1	< 1	3	ND	< 1	1	< 0	1	38
17-Jul-20	ND	< 1	1	< 1	2	3	23	< 1	6	1	< 0	3	3	7	3	< 1	3	54

* When LWC is not available, we consider mean LWC at PUY: 0.285 g m^{-3}
ND: Not determined
Concentrations lower than their standard deviation are preceded by the sign "<" (Standard deviation ≈ Limit of Quantification, see Figure S3, Table S3 and Section 3.1).

Table S1. Continued.

Label (dd.mm.yy)	Amino acids (µgC L^{-1})																
	Ala	*Arg*	*Asn*	*Asp*	*Gln*	*Glu*	*Gly*	*His*	*Leu / I*	*Lys*	*Met*	*Phe*	*Pro*	*Ser*	*Thr*	*Trp*	*Tyr*	***SUM***
22-Mar-14	7	3	< 1	4	< 2	13	3	6	14	8	2	1	4	8	4	3	4	**83**
3-May-18	8	< 2	1	4	0	2	5	1	5	0	0	3	9	12	5	< 1	3	**60**
13-Jun-18	3	< 3	37	< 2	< 2	2	3	< 3	7	< 3	< 2	< 3	5	3	1	< 3	< 3	**61**
24-Aug-18	11	2	48	5	6	7	7	3	9	1	< 2	7	8	11	11	3	3	**142**
24-Sep-18	4	2	4	1	0	3	4	2	4	1	< 0	2	4	6	8	1	1	**49**
1-Oct-18	28	< 2	11	16	1	9	13	10	23	4	< 0	7	16	54	17	1	13	**223**
8-Oct-18	11	< 2	1	5	< 1	3	6	1	12	< 1	< 0	3	7	12	6	1	3	**72**
25-Sep-19	ND	3	8	ND	2	4	28	ND	ND	4	< 2	12	ND	53	10	3	ND	**127**
2-Oct-19	ND	< 2	24	23	1	9	39	12	37	9	< 0	13	ND	97	20	1	16	**301**
22am-Oct-19	ND	< 2	1	8	< 1	4	15	4	12	3	< 0	4	ND	27	7	0	4	**89**
22pm-Oct-19	ND	1	0	2	< 1	1	18	1	9	< 1	0	3	ND	14	3	3	< 2	**56**
11-Mar-20	22	< 1	1	< 0	< 0	< 1	11	< 2	9	< 1	< 1	6	ND	< 1	1	< 1	1	**50**
17-Jul-20	ND	< 1	1	< 1	2	3	23	< 1	10	1	< 0	7	5	8	4	< 1	5	**69**

ND: Not determined
Concentrations lower than their standard deviation are preceded by the sign "<" (Standard deviation ≈ Limit of Quantification, see Figure S3, Table S3 and Section 3.1).

Table S1. Continued.

	Amino acids (relative abundance, % nM)*																
Label (dd.mm.yy)	***Ala***	***Arg***	***Asn***	***Asp***	***Gln***	***Glu***	***Gly***	***His***	***Leu / I***	***Lys***	***Met***	***Phe***	***Pro***	***Ser***	***Thr***	***Trp***	***Tyr***
22-Mar-14	13%	3%	*	6%	*	15%	7%	5%	13%	7%	2%	0%	5%	14%	6%	1%	3%
3-May-18	16%	*	1%	6%	1%	3%	16%	1%	6%	0%	1%	2%	12%	24%	8%	*	2%
13-Jun-18	7%	*	59%	*	*	3%	10%	*	7%	*	*	*	7%	6%	1%	*	*
24-Aug-18	10%	1%	34%	4%	4%	4%	10%	1%	4%	0%	*	2%	4%	11%	8%	1%	1%
24-Sep-18	12%	2%	8%	3%	1%	5%	18%	3%	5%	2%	*	2%	7%	15%	17%	0%	1%
1-Oct-18	16%	*	5%	7%	0%	3%	11%	3%	6%	1%	*	1%	5%	31%	7%	0%	2%
8-Oct-18	19%	*	1%	7%	*	4%	15%	1%	11%	*	*	2%	8%	22%	8%	0%	2%
25-Sep-19	ND	1%	5%	ND	1%	2%	35%	ND	ND	2%	*	3%	ND	44%	6%	1%	ND
2-Oct-19	ND	*	7%	7%	0%	2%	23%	2%	7%	2%	*	2%	ND	39%	6%	0%	2%
22am-Oct-19	ND	*	1%	8%	*	3%	30%	3%	8%	2%	*	2%	ND	35%	7%	0%	2%
22pm-Oct-19	ND	1%	1%	3%	*	1%	51%	1%	9%	*	0%	2%	ND	27%	4%	1%	*
11-Mar-20	48%	*	1%	*	*	*	35%	*	10%	*	*	4%	ND	*	2%	*	1%
17-Jul-20	ND	*	2%	*	2%	3%	56%	*	8%	1%	*	4%	5%	12%	4%	*	3%

*: Concentrations lower than their standard deviation (Standard deviation ≈ Limit of Quantification, see Figure S3, Table S3 and Section 3.1).

ND: Not determined

Table S1. Continued.

	Air mass history calculated with the CAT model*												
	Zone matrix				Sector matrix								
Label (dd.mm.yy)	Sea surface (<ABLH)¤	Sea surface (>ABLH)	Continental surface (<ABLH)	Continental surface (>ABLH)	SSW	WSW	WNW	NNW	NNE	ENE	ESE	SSE	NEAR
22-Mar-14	11.99%	76.38%	0.81%	10.82%	0.00%	77.37%	21.18%	0.00%	0.00%	0.00%	0.00%	0.00%	1.44%
3-May-18	10.74%	46.87%	0.88%	41.51%	0.00%	49.24%	26.28%	12.16%	9.71%	0.00%	0.00%	0.00%	2.61%
13-Jun-18	0.02%	40.33%	1.53%	58.13%	0.00%	0.00%	11.50%	56.40%	29.34%	0.00%	0.00%	0.00%	2.77%
24-Aug-18	27.26%	40.96%	6.63%	25.16%	0.00%	0.91%	96.68%	0.00%	0.00%	0.00%	0.00%	0.00%	2.41%
24-Sep-18	0.00%	55.88%	0.80%	43.31%	0.00%	0.00%	27.61%	30.30%	25.13%	15.02%	0.00%	0.00%	1.94%
1-Oct-18	27.41%	32.81%	11.21%	28.56%	0.00%	0.00%	60.44%	37.65%	0.00%	0.00%	0.00%	0.00%	1.91%
8-Oct-18	0.00%	7.44%	1.07%	91.50%	0.00%	0.00%	0.00%	0.00%	0.00%	55.94%	34.12%	5.73%	4.21%
25-Sep-19	48.82%	41.32%	0.00%	9.86%	0.00%	19.16%	79.53%	0.00%	0.00%	0.00%	0.00%	0.00%	1.31%
2-Oct-19	62.87%	4.55%	8.43%	24.15%	0.00%	7.57%	10.40%	55.43%	24.24%	0.00%	0.00%	0.00%	2.36%
22am-Oct-19	1.06%	35.76%	6.25%	56.94%	12.76%	5.88%	0.00%	0.00%	0.00%	0.00%	22.50%	56.69%	2.17%
22pm-Oct-19	0.00%	26.00%	8.95%	65.05%	4.50%	0.00%	0.00%	0.00%	0.00%	0.00%	20.25%	73.63%	1.62%
11-Mar-20	0.00%	86.48%	0.00%	13.52%	0.00%	67.70%	29.22%	0.00%	0.00%	0.00%	0.00%	0.00%	3.08%
17-Jul-20	0.00%	46.50%	0.00%	53.50%	0.00%	0.00%	51.20%	35.10%	10.50%	0.00%	0.00%	0.00%	3.20%

* Computing Atmospheric Trajectory Tool
¤ ABLH: Atmosphere Boundary Layer Height

Table S1. Continued.

	Physical characterization			Chemical characterization											Biological characterization	
Label (dd-mm-yy)	LWC (g m^{-3})	Effective Radius (µm)	Temp. (°C)	pH	Na^+ (µM)	NH_4^+ (µM)	Mg^{2+} (µM)	K^+ (µM)	Ca^{2+} (µM)	SO_4^{2-} (µM)	NO_3^- (µM)	Cl^- (µM)	TOC (mgC L^{-1})	H_2O_2 (µM)	Bacteria (17°C) CFU mL^{-1*}	ATP conc. (nM)
22-Mar-14	0.38	9.03	0	6.67	20.92	87.56	12.38	2.33	4.72	34.77	24.68	65.73	2.90	18.00	ND	ND
3-May-18	0.08	3.49	3	5.50	32.90	51.70	10.50	11.10	38.40	10.70	36.00	10.60	6.80	13.89	20	0.06
13-Jun-18	ND	ND	6.9	5.00	22.70	125.60	10.60	4.10	49.30	6.20	30.60	15.40	10.60	29.26	150	0.12
24-Aug-18	ND	ND	10.3	5.00	22.80	17.30	6.50	11.70	42.50	13.60	76.10	13.20	7.20	6.28	235	0.21
24-Sep-18	ND	ND	2.4	4.70	14.20	21.40	5.70	6.20	40.50	9.60	32.80	4.50	3.00	2.95	216	0.01
1-Oct-18	0.06	2.94	0.8	5.00	30.20	21.30	14.20	7.40	61.00	26.60	37.20	11.80	6.70	0.72	340	0.03
8-Oct-18	0.17	2.75	8	4.50	21.40	78.90	8.60	7.10	52.40	15.30	132.00	26.40	9.80	14.64	277	0.05
25-Sep-19	ND	ND	6.8	5.21	105.26	3.00	7.56	15.42	10.59	14.34	6.14	114.18	6.90	19.20	179	0.68
2-Oct-19	ND	ND	6.1	5.15	120.38	4.18	7.48	39.01	19.35	13.23	42.60	108.97	6.80	5.75	212	0.84
22am-Oct-19	ND	ND	5.8	5.80	68.66	0.00	3.90	14.17	7.44	11.69	10.04	52.01	3.20	34.65	134	0.40
22pm-Oct-19	ND	ND	6.3	5.80	46.09	0.00	4.23	13.85	9.61	19.67	0.10	35.12	11.20	31.64	120	0.34
11-Mar-20	ND	ND	5.7	5.13	53.02	61.75	4.13	16.48	6.03	21.51	12.83	37.78	4.00	0.50	186	0.30
17-Jul-20	0.07	11.20	10.3	5.44	54.66	339.76	13.25	12.61	36.23	39.99	162.06	39.62	ND	ND	196	2.25

*CFU: Colony-Forming Unit

Table S2. Retention times and exact mass of the AA measured by UPLC-HRMS in cloud samples.

Amino Acid	Abbrev.	Molecular formula	Monoisotopic mass (Da)	m/z $[M+H]^+$	Mean retention time (min)
Alanine	Ala	$C_3H_7NO_2$	89.0477	90.0557	3.66
Arginine	Arg	$C_6H_{14}N_4O_2$	174.1117	175.1194	6.84
Asparagine	Asn	$C_4H_8N_2O_3$	132.0535	133.0612	5.3
Aspartic acid	Asp	$C_4H_7NO_4$	133.0375	134.0452	4.92
Glutamine	Gln	$C_5H_{10}N_2O_3$	146.0691	147.0768	5.13
Glutamic acid	Glu	$C_5H_8NO_4$	147.0532	148.0608	4.47
Glycine	Gly	$C_2H_5NO_2$	75.0320	76.0401	4.14
Histidine	His	$C_6H_9N_3O_2$	155.0695	156.0772	6.95
Isoleucine	Ile	$C_6H_{13}NO_2$	131.0946	132.1023	1.66
Leucine	Leu	$C_6H_{13}NO_2$	131.0946	132.1023	1.66
Lysine	Lys	$C_6H_{14}N_2O_2$	146.1055	147.1127	6.77
Methionine	Met	$C_5H_{11}NO_2S$	149.0511	150.0588	2.79
Phenylalanine	Phe	$C_9H_{11}NO_2$	165.0790	166.0867	2.33
Proline	Pro	$C_5H_9NO_2$	115.0633	116.0711	4.19
Serine	Ser	$C_3H_7NO_3$	105.0426	106.0504	5.14
Threonine	Thr	$C_4H_9NO_3$	119.0582	120.0660	4.43
Tryptophan	Trp	$C_{11}H_{12}N_2O_2$	204.0899	205.0978	2.00
Tyrosine	Tyr	$C_9H_{11}NO_3$	181.0739	182.0815	3.65
Valine	Val	$C_5H_{11}NO_2$	117.0790	118.0868	2.85

Table S3. Concentration (µg L^{-1} with dilution 9:1, detailed in Figure S3), calibration curve and R^2 data for the 18 amino acids (AA) analyzed in the 13 clouds sampled at PUY. The calculation method (detailed in Figure S3) might mathematically provide negative values for the concentration. Approximating the limit of quantification by the standard deviation of the measurements (STD_M), amino acids with an average concentration lower than STD_M are considered unquantifiable. ND: Not Determined. The p-values of all the correlations are strictly less than 0.05.

22-Mar-14					
AA	Concentration (µg L^{-1})			Eq. of calibration curve	R²
Ala	17	±	4	y = 9.6E+4 x + 1.7E+6	0.9984
Arg	8	±	1	y = 3.7E+5 x + 3.0E+6	0.9999
Asn	-1	±	4	y = 8.0E+4 x - 9.8E+4	0.9977
Asp	12	±	3	y = 5.2E+4 x + 6.1E+5	0.9989
Gln	-4	±	4	y = 1.1E+5 x - 4.8E+5	0.9984
Glu	32	±	9	y = 1.7E+5 x + 5.4E+6	0.9916
Gly	8	±	2	y = 1.2E+5 x + 9.6E+5	0.9997
His	12	±	4	y = 3.4E+5 x + 4.1E+6	0.9985
Leu/I	26	±	7	y = 3.3E+5 x + 8.4E+6	0.9943
Lys	16	±	7	y = 7.7E+4 x + 1.2E+6	0.9970
Met	4	±	3	y = 2.8E+5 x + 1.0E+6	0.9989
Phe	0.9	±	0.8	y = 4.8E+5 x + 4.6E+5	0.9999
Pro	8	±	2	y = 4.6E+5 x + 3.6E+6	0.9993
Ser	22	±	9	y = 1.1E+5 x + 2.5E+6	0.9911
Thr	11	±	4	y = 8.6E+4 x + 9.8E+5	0.9983
Trp	4	±	3	y = 1.5E+5 x + 6.1E+5	0.9984
Tyr	7	±	3	y = 2.0E+5 x + 1.4E+6	0.9985

3-May-18					
AA	Concentration (µg L^{-1})			Eq. of calibration curve	R²
Ala	19	±	1	y = 7.6E+4 x + 1.5E+6	0.9998
Arg	-4	±	4	y = 3.8E+5 x - 1.4E+6	0.9974
Asn	2.0	±	0.4	y = 9.0E+4 x + 1.8E+5	1.0000
Asp	11	±	2	y = 4.6E+4 x + 5.1E+5	0.9994
Gln	1.0	±	0.7	y = 1.6E+5 x + 1.6E+5	0.9999
Glu	6	±	1	y = 1.2E+5 x + 7.2E+5	0.9998
Gly	16	±	2	y = 1.1E+5 x + 1.8E+6	0.9996
His	3	±	1	y = 3.7E+5 x + 1.2E+6	0.9998
Leu/I	10	±	1	y = 3.4E+5 x + 3.3E+6	0.9998
Lys	0	±	2	y = 8.0E+4 x + 1.9E+3	0.9996
Met	0.5	±	0.6	y = 2.6E+5 x + 1.5E+5	1.0000
Phe	5	±	2	y = 4.3E+5 x + 2.2E+6	0.9995
Pro	18	±	2	y = 3.6E+5 x + 6.5E+6	0.9995
Ser	34	±	5	y = 1.1E+5 x + 3.9E+6	0.9982
Thr	13	±	2	y = 8.5E+4 x + 1.1E+6	0.9996
Trp	-1	±	1	y = 1.7E+5 x - 1.4E+5	1.0000
Tyr	5	±	1	y = 1.7E+5 x + 8.0E+5	0.9998

13-Jun-18					
AA	Concentration (µg L^{-1})			Eq. of calibration curve	R²
Ala	8	±	5	y = 1.9E+4 x + 1.5E+5	0.9981
Arg	-2	±	7	y = 4.1E+5 x - 1.0E+6	0.9954
Asn	102	±	4	y = 4.5E+4 x + 4.6E+6	0.9995
Asp	4	±	5	y = 2.1E+4 x + 8.3E+4	0.9977
Gln	-1	±	5	y = 9.9E+4 x - 1.3E+5	0.9975
Glu	2	±	5	y = 7.9E+4 x + 1.9E+5	0.9971
Gly	10	±	6	y = 4.5E+4 x + 4.3E+5	0.9949
His	-4	±	6	y = 3.8E+5 x - 1.6E+6	0.9976
Leu/I	12	±	4	y = 1.8E+5 x + 2.2E+6	0.9983
Lys	-5	±	6	y = 5.6E+4 x - 2.8E+5	0.9965
Met	-6	±	6	y = 1.7E+5 x - 1.1E+6	0.9977
Phe	-2	±	4	y = 3.6E+5 x - 8.7E+5	0.9982
Pro	10	±	5	y = 3.3E+5 x + 3.2E+6	0.9980
Ser	8	±	5	y = 5.5E+4 x + 4.2E+5	0.9979
Thr	2	±	4	y = 4.6E+4 x + 1.2E+5	0.9983
Trp	-4	±	5	y = 1.1E+5 x - 4.7E+5	0.9977
Tyr	-4	±	5	y = 1.3E+5 x - 4.7E+5	0.9975

24-Aug-18					
AA	Concentration (µg L^{-1})			Eq. of calibration curve	R²
Ala	26	±	2	y = 2.4E+4 x + 6.2E+5	0.9994
Arg	5	±	3	y = 2.8E+5 x + 1.5E+6	0.9992
Asn	130	±	17	y = 5.8E+4 x + 7.6E+6	0.9899
Asp	15	±	4	y = 1.5E+4 x + 2.3E+5	0.9979
Gln	15	±	5	y = 5.9E+4 x + 8.7E+5	0.9964
Glu	17	±	11	y = 5.6E+4 x + 9.6E+5	0.9894
Gly	21	±	4	y = 3.4E+4 x + 7.2E+5	0.9978
His	6	±	1	y = 2.3E+5 x + 1.3E+6	0.9999
Leu/I	17	±	3	y = 1.4E+5 x + 2.4E+6	0.9990
Lys	2	±	1	y = 3.3E+4 x + 7.0E+4	0.9999
Met	-1	±	4	y = 1.2E+5 x - 1.8E+5	0.9978
Phe	11	±	5	y = 2.2E+5 x + 2.5E+6	0.9968
Pro	15	±	3	y = 2.5E+5 x + 3.9E+6	0.9987
Ser	33	±	5	y = 4.0E+4 x + 1.3E+6	0.9975
Thr	28	±	4	y = 3.3E+4 x + 9.3E+5	0.9981
Trp	3.7	±	0.9	y = 6.3E+4 x + 2.3E+5	0.9999
Tyr	5	±	4	y = 7.9E+4 x + 4.1E+5	0.9979

24-Sep-18					
AA	Concentration ($\mu g\ L^{-1}$)			Eq. of calibration curve	R^2
Ala	10.7	±	0.6	y = 2.8E+4 x + 3.0E+5	0.9987
Arg	4.3	±	0.8	y = 2.2E+5 x + 9.5E+5	0.9985
Asn	11	±	2	y = 4.2E+4 x + 4.7E+5	0.9994
Asp	4.4	±	0.6	y = 1.9E+4 x + 8.3E+4	0.9988
Gln	1.0	±	0.6	y = 6.7E+4 x + 6.5E+4	0.9989
Glu	6.8	±	0.8	y = 6.4E+4 x + 4.4E+5	0.9977
Gly	14.2	±	0.6	y = 3.8E+4 x + 5.4E+5	0.9989
His	5	±	1	y = 2.6E+5 x + 1.4E+6	0.9964
Leu/I	7.1	±	0.8	y = 1.6E+5 x + 1.1E+6	0.9978
Lys	3.4	±	0.8	y = 3.4E+4 x + 1.2E+5	0.9981
Met	0.4	±	0.7	y = 1.5E+5 x + 5.9E+4	0.9983
Phe	3	±	1.1	y = 3.0E+5 x + 9.9E+5	0.9953
Pro	8.4	±	1.0	y = 3.2E+5 x + 2.7E+6	0.9968
Ser	17.3	±	0.8	y = 4.9E+4 x + 8.5E+5	0.9976
Thr	20.7	±	1.0	y = 4.0E+4 x + 8.2E+5	0.9970
Trp	0.9	±	0.6	y = 7.7E+4 x + 7.3E+4	0.9986
Tyr	2.2	±	0.8	y = 1.1E+5 x + 2.4E+5	0.9975

1-Oct-18					
AA	Concentration ($\mu g\ L^{-1}$)			Eq. of calibration curve	R^2
Ala	69	±	5	y = 3.0E+4 x + 2.1E+6	0.9978
Arg	1	±	6	y = 4.1E+5 x + 2.5E+5	0.9952
Asn	31	±	7	y = 4.2E+4 x + 1.3E+6	0.9960
Asp	45	±	7	y = 2.1E+4 x + 9.4E+5	0.9950
Gln	3	±	1	y = 7.9E+4 x + 2.6E+5	0.9998
Glu	22	±	3	y = 7.4E+4 x + 1.6E+6	0.9988
Gly	42	±	2	y = 4.3E+4 x + 1.8E+6	0.9993
His	22	±	4	y = 3.0E+5 x + 6.7E+6	0.9980
Leu/I	41	±	4	y = 1.6E+5 x + 6.3E+6	0.9983
Lys	9	±	4	y = 4.9E+4 x + 4.5E+5	0.9981
Met	-0	±	1	y = 1.7E+5 x - 6.5E+4	0.9998
Phe	10	±	3	y = 3.5E+5 x + 3.5E+6	0.9989
Pro	30	±	3	y = 3.3E+5 x + 9.9E+6	0.9991
Ser	157	±	8	y = 5.4E+4 x + 8.5E+6	0.9974
Thr	42	±	2	y = 4.5E+4 x + 1.9E+6	0.9995
Trp	2	±	1	y = 8.4E+4 x + 1.5E+5	0.9998
Tyr	21	±	5	y = 1.1E+5 x + 2.2E+6	0.9972

8-Oct-18					
AA	Concentration ($\mu g\ L^{-1}$)			Eq. of calibration curve	R^2
Ala	27	±	2	y = 7.5E+4 x + 2.1E+6	0.9996
Arg	-4	±	6	y = 4.0E+5 x - 1.6E+6	0.9952
Asn	1.5	±	1.0	y = 9.7E+4 x + 1.5E+5	0.9999
Asp	13.7	±	0.3	y = 5.2E+4 x + 7.1E+5	1.0000
Gln	0	±	2	y = 1.7E+5 x + 4.7E+4	0.9994
Glu	8	±	3	y = 1.3E+5 x + 1.1E+6	0.9988
Gly	18.0	±	0.6	y = 1.2E+5 x + 2.2E+6	1.0000
His	3	±	2	y = 4.0E+5 x + 1.0E+6	0.9996
Leu/I	21.6	±	0.7	y = 3.5E+5 x + 7.6E+6	0.9999
Lys	-1	±	3	y = 8.3E+4 x - 8.8E+4	0.9988
Met	-0.7	±	0.6	y = 2.9E+5 x - 2.2E+5	1.0000
Phe	5	±	1	y = 4.6E+5 x + 2.3E+6	0.9998
Pro	14.2	±	0.9	y = 3.9E+5 x + 5.6E+6	0.9999
Ser	36	±	1	y = 1.3E+5 x + 4.6E+6	0.9999
Thr	15	±	1	y = 8.9E+4 x + 1.4E+6	0.9998
Trp	0.6	±	0.5	y = 1.7E+5 x + 9.5E+4	1.0000
Tyr	5	±	3	y = 1.9E+5 x + 1.0E+6	0.9984

25-Sep-19					
AA	Concentration ($\mu g\ L^{-1}$)			Eq. of calibration curve	R^2
Ala				ND	
Arg	8	±	4	y = 2.5E+4 x + 2.0E+5	0.9831
Asn	21	±	3	y = 6.2E+3 x + 1.3E+5	0.9778
Asp				ND	
Gln	6	±	2	y = 9.7E+3 x + 6.2E+4	0.9965
Glu	10	±	1	y = 9.2E+3 x + 9.6E+4	0.9957
Gly	87	±	8	y = 1.6E+3 x + 1.4E+5	0.9781
His				ND	
Leu/I				ND	
Lys	8	±	1	y = 7.6E+3 x + 6.2E+4	0.9978
Met	-7	±	3	y = 4.1E+3 x - 2.8E+4	0.9566
Phe	18	±	5	y = 2.3E+4 x + 4.2E+5	0.9783
Pro				ND	
Ser	150	±	22	y = 4.1E+3 x + 6.3E+5	0.9384
Thr	25	±	3	y = 6.0E+3 x + 1.5E+5	0.9918
Trp	5	±	2	y = 3.7E+3 x + 1.8E+4	0.9488
Tyr				ND	

2-Oct-19					
AA	Concentration ($\mu g\ L^{-1}$)			Eq. of calibration curve	R^2
Ala	ND				
Arg	3	±	4	y = 2.7E+5 x + 7.4E+5	0.9978
Asn	67.3	±	0.9	y = 1.5E+4 x + 1.0E+6	0.9999
Asp	65	±	2	y = 7.2E+3 x + 4.7E+5	0.9994
Gln	2.43	±	2	y = 2.4E+4 x + 5.9E+4	0.9994
Glu	22.0	±	0.9	y = 2.5E+4 x + 5.6E+5	0.9999
Gly	121	±	3	y = 4.6E+3 x + 5.5E+5	0.9994
His	25.9	±	0.7	y = 1.5E+5 x + 3.8E+6	0.9999
Leu/I	68	±	1	y = 5.3E+4 x + 3.6E+6	0.9998
Lys	19	±	1	y = 3.8E+4 x + 7.1E+5	0.9997
Met	-0	±	1	y = 3.5E+4 x - 6.4E+3	0.9998
Phe	19.7	±	0.3	y = 1.2E+5 x + 2.3E+6	0.9999
Pro	ND				
Ser	282	±	6	y = 1.5E+4 x + 4.3E+6	0.9985
Thr	49	±	1	y = 1.3E+4 x + 6.5E+5	0.9998
Trp	1.0	±	0.2	y = 4.1E+4 x + 4.1E+4	0.9999
Tyr	27	±	3	y = 3.3E+4 x + 8.9E+5	0.9984

22am-Oct-19					
AA	Concentration ($\mu g\ L^{-1}$)			Eq. of calibration curve	R^2
Ala	ND				
Arg	-2	±	4	y = 2.6E+5 x - 4.7E+5	0.9973
Asn	2.3	±	0.6	y = 1.4E+4 x + 3.2E+4	0.9999
Asp	21.8	±	1.0	y = 6.4E+3 x + 1.4E+5	0.9998
Gln	-2	±	2	y = 2.1E+4 x - 4.0E+4	0.9992
Glu	9.7	±	0.7	y = 2.4E+4 x + 2.3E+5	0.9999
Gly	48	±	2	y = 4.0E+3 x + 1.9E+5	0.9994
His	8.7	±	0.5	y = 1.3E+5 x + 1.1E+6	0.9999
Leu/I	21.5	±	0.5	y = 6.9E+4 x + 1.5E+6	1.0000
Lys	6	±	1	y = 3.4E+4 x + 2.2E+5	0.9996
Met	-2.0	±	0.6	y = 3.6E+4 x - 7.2E+4	1.0000
Phe	6.19	±	0.37	y = 1.4E+5 x + 8.4E+5	0.9997
Pro	ND				
Ser	78	±	2	y = 1.5E+4 x + 1.2E+6	0.9995
Thr	18.1	±	0.7	y = 1.2E+4 x + 2.2E+5	0.9999
Trp	-0.2	±	0.3	y = 4.4E+4 x - 9.0E+3	1.0000
Tyr	7	±	2	y = 3.2E+4 x + 2.4E+5	0.9996

22pm-Oct-19					
AA	Concentration ($\mu g\ L^{-1}$)			Eq. of calibration curve	R^2
Ala	ND				
Arg	2.2	±	0.6	y = 1.8E+5 x + 4.0E+5	0.9992
Asn	1.0	±	0.4	y = 1.4E+4 x + 1.3E+4	1.0000
Asp	6	±	1	y = 6.6E+3 x + 4.2E+4	0.9998
Gln	-2	±	2	y = 2.1E+4 x - 4.6E+4	0.9994
Glu	2.8	±	0.5	y = 2.4E+4 x + 6.6E+4	1.0000
Gly	57	±	5	y = 3.5E+3 x + 2.0E+5	0.9966
His	3.4	±	1.0	y = 1.3E+5 x + 4.4E+5	0.9998
Leu/I	17	±	3	y = 6.9E+4 x + 1.2E+6	0.9983
Lys	1	±	2	y = 3.3E+4 x + 3.8E+4	0.9995
Met	-1.3	±	0.4	y = 4.0E+4 x - 5.2E+4	1.0000
Phe	4	±	1	y = 1.5E+5 x + 6.4E+5	0.9961
Pro	ND				
Ser	42	±	1	y = 1.5E+4 x + 6.3E+5	0.9998
Thr	8.0	±	0.5	y = 1.2E+4 x + 9.5E+4	1.0000
Trp	4	±	3	y = 4.3E+4 x + 1.8E+5	0.9985
Tyr	-1	±	3	y = 3.2E+4 x - 1.7E+4	0.9983

11-Mar-20					
AA	Concentration ($\mu g\ L^{-1}$)			Eq. of calibration curve	R^2
Ala	54	±	10	y = 1.5E+3 x + 8.0E+4	0.9906
Arg	3	±	3	y = 1.4E+5 x + 3.9E+5	0.9894
Asn	2.3	±	0.9	y = 1.0E+4 x + 2.3E+4	0.9998
Asp	-2	±	1	y = 1.8E+3 x - 4.4E+3	0.9996
Gln	-0.5	±	0.6	y = 1.8E+4 x - 9.1E+3	0.9995
Glu	1	±	2	y = 1.4E+4 x + 1.1E+4	0.9993
Gly	33	±	3	y = 4.1E+2 x + 1.4E+4	0.9986
His	2	±	4	y = 1.1E+5 x + 2.6E+5	0.9970
Leu/I	15.6	±	0.7	y = 4.4E+4 x + 6.8E+5	0.9999
Lys	-1	±	2	y = 3.8E+4 x - 5.1E+4	0.9994
Met	-10	±	2	y = 2.3E+4 x - 2.3E+5	0.9995
Phe	9	±	2	y = 5.3E+4 x + 4.6E+5	0.9995
Pro	ND				
Ser	0	±	3	y = 5.1E+3 x + 1.8E+3	0.9989
Thr	3	±	3	y = 6.9E+3 x + 2.4E+4	0.9983
Trp	-1	±	1	y = 3.5E+4 x - 1.8E+4	0.9996
Tyr	2	±	2	y = 1.7E+4 x + 3.6E+4	0.9990

17-Jul-20					
AA	Concentration ($\mu g\ L^{-1}$)			Eq. of calibration curve	R^2
Ala			ND		
Arg	2	±	2	y = 1.8E+4 x + 2.9E+4	0.9971
Asn	4	±	1	y = 2.6E+3 x + 1.1E+4	0.9991
Asp	-1	±	2	y = 8.6E+2 x - 8.4E+2	0.9983
Gln	6	±	1	y = 4.8E+3 x + 2.8E+4	0.9988
Glu	8	±	1	y = 4.5E+3 x + 3.8E+4	0.9987
Gly	72	±	8	y = 3.8E+2 x + 2.7E+4	0.9829
His	-2	±	2	y = 1.5E+4 x - 3.8E+4	0.9979
Leu/I	19	±	1	y = 5.6E+3 x + 1.1E+5	0.9985
Lys	2	±	1	y = 4.4E+3 x + 6.7E+3	0.9985
Met	-2	±	1	y = 5.8E+3 x - 1.0E+4	0.9991
Phe	9.8	±	0.9	y = 1.3E+4 x + 1.2E+5	0.9994
Pro	9.4	±	0.6	y = 3.4E+4 x + 3.1E+5	0.9997
Ser	22	±	3	y = 1.9E+3 x + 4.3E+4	0.9960
Thr	9	±	1	y = 3.0E+3 x + 2.7E+4	0.9989
Trp	-5	±	2	y = 6.3E+3 x - 2.9E+4	0.9980
Tyr	8	±	2	y = 4.2E+3 x + 3.5E+4	0.9981

Table S4. FAAs concentrations in atmospheric samples: Cloud, fog, rain and aerosol particles (non-exhaustive).

Localization	Environment	Period / Samples	Method Separation	Concentration range FAAs	Distribution (major FAAs)	Reference
Cloud, fog, rain						
Puy de Dôme Mountain, France (1465 m)	Rural + marine influence (Cloud)	03/2014 05-10/2018 09, 10/2019 03, 07/2020 13 samples	HPLC-MS/MS Standard addition	Range: 39 - 244 ng m^{-3}	Ser > Gly > Ala > Asn > Leu/I	This work
Puy de Dôme Mountain, France (1465 m)	Rural + marine influence (Cloud)	03-04/2014 (spring) 11/2014 (winter) 25 samples	HPLC-Fluorescence OPA-Derivatization	Mean: 118.6 ± 97.6 ng m^{-3}	Trp > Ile/Leu > Phe > Ser	Bianco et al. (2016)
Cape Verde Islands (744 m)	Marine (Cloud)	09-10/2017 (winter) 10 samples	HPLC-MS Waters AccQ-Tag-Derivatization	Range: 11.2 - 489.9 ng m^{-3}	Ser > Asp > Ala > Gly > Thr	Triesch et al. (2021)
Davis, CA, US (10 m)	Rural (Fog)	1997 - 1999 (winter) 11 samples	HPLC-Fluorescence OPA-Derivatization	Mean: 40.8 ± 38.0 ng m^{-3} (FAAs, protein type)	Ser > Gly > Leu > Ala > Val	Zhang and Anastasio (2003)
Atlantic Ocean, Golf Mexico (Cruise)	Marine (Rain)	09-10/1985 02, 06, 09/1986 7 samples	HPLC-Fluorescence OPA-Derivatization	Mean: 604 ± 585 µg L^{-1}	Gly > Ser > Ala > acidic AAs	Mopper and Zika (1987)
Seoul, South Korea (17 m) Uljin, South Korea (30 m)	Urban (Rain) Marine (Rain)	03/2012 - 04/2014 36 samples 02/2011 - 01/2012 31 samples	HPLC-Fluorescence OPA-Derivatization	Mean: 21.0 ± 17.9 µg L^{-1} (Seoul) Mean: 100.9 ± 110.2 µg L^{-1} (Uljin)	Gly > Glu > Asp > Ser	Yan et al. (2015)
Guiyang, China (1300 m)	Suburban (Rain)	05/2017 - 04/2018 Summer (n = 29) Autumn (n = 9) Winter (n = 14) Spring (n = 13) 65 samples	HPLC-Fluorescence OPA-Derivatization	Total: 1.1 - 10.1 µM Mean: 3.7 µM Range Summer: 1.3 - 6.6 µM Mean Summer: 2.9 µM Range Autumn: 1.1 - 8.8 µM Mean Autumn: 4.4 µM Range Winter: 1.5 - 9.9 µM Mean Winter: 3.4 µM Range Spring: 2.6 - 10.1 µM Mean Spring: 5.2 µM	Glu + Gln, Gly, Pro > Asp, Ala	Xu et al. (2019)

Aerosol						
Erdemli, Eastern Mediterranean coast, Turkey (21m)	Marine (Aerosol)	03-05/2000 (spring) 39 samples	HPLC-UV-Vis DABS-Cl- Derivatization	Mean: 33.8 ng m^{-3} Range: 3.65 - 102 ng m^{-3}	Gly > Arg > Val > Pro	Mace et al. (2003a)
Cape Grim Baseline Air, Tasmania (94 m)	Marine (Aerosol)	11/2000 (winter) 13 samples	HPLC-UV-Vis DABS-Cl- Derivatization	Mean: 8.74 ng m^{-3} Range: 1.83 - 20 ng m^{-3}	Arg > Gly > Pro > Ala > Val	Mace et al. (2003b)
Davis, CA, US (10 m)	Rural (Aerosol)	08/1997 - 07/1998 41 PM$_{2.5}$ samples	HPLC-Fluorescence OPA-Derivatization	Mean: 58.5 ng m^{-3} Range: 8.62 - 236 ng m^{-3}	Ornithine > Gly > Thr > Ser > Ala	Zhang and Anastasio (2003)
Western Pacific Ocean (Cruise)	Marine (Aerosol)	05-06/2000 (spring) 06-07/2000 (summer) Fine p. d < 2.5 µm Coarse p. d > 2.5 µm 15 samples	HPLC-Fluorescence OPA-Derivatization	Mean: 0.98 ng m^{-3} Range: 0.14 - 2.81 ng m^{-3}	Gly > Ser > Asp > Ala	Matsumoto and Uematsu (2005)
Atlantic (Cruise)	Marine (Aerosol)	05-06/2003 (spring) Total suspended particles	HPLC-Fluorescence OPA-Derivatization	Mean: 1.83 ng m^{-3} Range: 0.27 - 9.13 ng m^{-3}	Gly > Ala > Ser > Leu	Wedyan and Preston (2008)
Finokalia, Crete Island, Greece (250 m)	Marine (Aerosol)	7/2007-8/2010 (summer/autumn) 47 daily PM$_1$ samples	HPLC-UV/Vis DABS-Cl- Derivatization	Mean: 45.6 ng m^{-3}	Gly > Ser > Arg + Ala > Lys > His	Violaki and Mihalopoulos (2010)
Finokalia, Crete Island, Greece (250 m)	Marine (Aerosol)	06-08/2007 (summer) 46 samples Total suspended particles	GC-MS MTBSTFA- Derivatization	Mean: 16.01 ng m^{-3} Range: 0.7 - 76.9 ng m^{-3}	Gly > Gln > Ala > Asp ∽ Glu	Mandalakis et al. (2011)
CVAO (0 m) Mt Verde (744m) Island of São Vicente, Cape Verde	Marine (Aerosol)	09-10/2017 (autumn) 8 samples 5 size segregated aerosol particles (0.05 - 10 µm)	HPLC-MS/MS	CVAO: Range PM$_{1.2}$: 1.3 - 6.3 ng m^{-3} Range PM$_{>1.2}$: 0.2 - 1.4 ng m^{-3} MV: Range PM$_{1.2}$: 0.8 - 1.9 ng m^{-3} Range PM$_{>1.2}$: 0.2 - 2.9 ng m^{-3}	Gly > Ala > Ser CVAO & MV	Triesch et al. (2021)

Gosan, Jeju Island, South Korea (10 m)	Rural (Aerosol)	03-04/2001 (spring) $PM_{2.5}$ 36 samples 4 composites (9 samples grouped together)	HPLC-Fluorescence OPA-Derivatization	Range TAAs: 77 - 255 ng m^{-3} FAA ~ 19% TAA	Gly > Glu > Val	Yang et al. (2004)
Duke Forest Research Facility NC, USA (150 m)	Rural (Aerosol)	07-08/2010 (summer) $PM_{2.5}$ 13 samples	HPLC-MS	Range: 11 - 40 ng m^{-3}	Gly > Arg > Ala > Asp > Glu	Samy et al. (2011)
SMEAR II station, Hyytiälä, Finland (148 m)	Rural (Aerosol)	02-10/2014 Dekati PM_{10} cascade impactor (<1.0, 1-2.5, 2.5-10 and >10 µm) 69 samples	HPLC-MS/MS	Mean: PM_1: 5.22 ng m^{-3} $PM_{2.5}$: 10.95 ng m^{-3} PM_{10}: 18.45 ng m^{-3} $PM_{>10}$: 27.62 ng m^{-3}	PM_1: Arg > Gly > Pro $PM_{2.5}$: Arg > Pro > Gln PM_{10}: Arg > Pro > Gln $PM_{>10}$: Pro > Arg > Gly	Helin et al. (2017)
Tianhu, Guangzhou, China (170 m)	Rural (Aerosol)	03/2012 - 02/2013 $PM_{2.5}$ 52 samples	HPLC-Fluorescence OPA-Derivatization	Mean: Annual: 133 ± 48 ng m^{-3} Spring: 107 ± 26 ng m^{-3} Summer: 115 ± 35 ng m^{-3} Autumn: 186 ± 56 ng m^{-3} Winter: 123 ± 31 ng m^{-3}	Gly > Val > Met > Phe	Song et al. (2017)
Col Margherita Atmospheric Observatory, Eastern Alps, Italy (2543 m)	Remote (Aerosol)	04, 08/2018 (spring/summer) PM_{10} 7 samples	HPLC-MS/MS	Mean spring: 6 ± 5 ng m^{-3} Mean summer 7 ± 2 ng m^{-3}	Spring: Gly > Glu > Arg Summer: Gly > Glu > Ala	Barbaro et al. (2020)
SMEAR II station, Hyytiälä, Finland (148 m)	Rural (Aerosol)	09-11/2017 Cascade impactor (PM_1 to PM_{10}) 84 samples	HPLC-MS/MS	Range PM_1: 2.1 - 5.4 ng m^{-3} Range $PM_{2.5}$: 1.8 - 5.7 ng m^{-3} Range PM_{10}: 11.4 - 36.9 ng m^{-3} Range $PM_{>10}$: 7.1 - 46.6 ng m^{-3}	PM_1: Gly > Ala > Glu $PM_{2.5}$: Gln > Arg > Glu PM_{10}: Leu > Arg > Gln $PM_{>10}$: Leu > Asp > Arg	Ruiz-Jimenez et al. (2021)

Nanjing University, China (10 m) Purple Mountain Observatory, Nanjing, China (267 m)	Urban (Aerosol) Suburban (Aerosol)	02/2001 (winter) - 09/2001 (autumn) $PM_{2.5}$ 10 samples (winter) 14 samples (autumn) 02/2001 (winter) $PM_{2.5}$ 12 samples	HPLC-Fluorescence AQC-Derivatization	Mean: 129 ng m^{-3} (winter) Range: 81.9 - 188 ng m^{-3} Mean: 84.9 ng m^{-3} (autumn) Range: 39.3 - 162 ng m^{-3} Mean: 189 ng m^{-3} (winter) Range: 58.5 - 396 ng m^{-3}	Gly > Cys > Val	Yang et al. (2005)
Sacca San Biagio Island, Venice, Italy (0 m)	Urban (Aerosol)	04-10/2007 Total suspended particles 10 samples	HPLC-MS/MS	Mean: 38 ng m^{-3} Range FAAs: 7 - 146 ng m^{-3}	Gly > Gln > Pro > Ala Asn > Glu > Asp > Ser	Barbaro et al. (2011)
Research Triangle Park NC, US (90 m)	Suburban (Aerosol)	09-10/2010 $PM_{2.5}$ (30 samples)	HPLC-MS/MS	Mean: 11 ± 6 ng m^{-3}	Gly > Ala = Asp = Arg > Glu > Ser	Samy et al. (2013)
University of Rome, Italy (40 m)	Urban (Aerosol)	01/2013 (winter) - 09/2013 (summer) $PM_{0.1}$, PM_1, $PM_{2.5}$, PM_{10} 13 samples (winter) 13 samples (summer)	HPLC-MS/MS	Mean: PM_{10}:195 ng m^{-3} (winter) 272 ng m^{-3} (summer) $PM_{2.5}$: 167 ng m^{-3} (winter) 193 ng m^{-3} (summer) PM_1: 129 ng m^{-3} (winter) 145 ng m^{-3} (summer) $PM_{0.1}$: 48 ng m^{-3} (winter) 94 ng m^{-3} (summer)	Gly > Ser > His > Asp	Di Filippo et al. (2014)
Institute of Atmospheric, Physics, Beijing, China (50 m)	Urban (Aerosol)	04-05/2013 (spring) Total suspended particles 29 samples	HPLC-Fluorescence OPA-Derivatization	Range TAAs: Whole year: 72 - 3820 ng m^{-3} Spring: 374 - 3195 ng m^{-3} Summer: 154 - 2262 ng m^{-3} Fall: 161 - 2067 ng m^{-3} Winter: 340 - 2405 ng m^{-3} *FAA ~ 25 % TAA*	Gly > Ala > Val	Ren et al. (2018)
Nanchang, China (37 m)	Urban Town Suburban Airport Forested site (Aerosol)	04-05/2019 $PM_{2.5}$ 14 samples / site	GC-MS tBDMS-Derivatization	Range total FAAs: 57 - 1238 pmol m^{-3} Mean: Airport: 321 ± 200 pmol m^{-3} Town: 350 ± 267 pmol m^{-3} Urban: 307 ± 131 pmol m^{-3} Suburban: 264 ± 113 pmol m^{-3} Forest: 220 ± 132 pmol m^{-3}	Gly > Ala = Pro	Zhu et al. (2021)

Gruvenbadet observatory, Svalbard, Arctic (8 m)	Polar (Aerosol)	04-09/2010 (boreal summer) Cascade impactor 9 samples	HPLC-MS/MS	Mean $PM_{0.5}$: 102.42 ng m^{-3} Range: 15.66 - 308.65 ng m^{-3}	Gly > Ser > Ala	Scalabrin et al. (2012)
Faraglione Camp, MZS, Antarctica (57 m)	Polar coastal area (Aerosol)	11/2010-01/2011 (summer) PM_{10} and cascade impactor 5 samples	HPLC-MS/MS	Mean: PM_{10}: 1.51 ng m^{-3} Mean: PM_1: 1.5 ng m^{-3}	Arg > Gly	Barbaro et al. (2015)
Dome C station, Antarctic (3233m)	Polar (Aerosol)	11/2011-01/2012 (summer) PM_{10} and cascade impactor 4 samples		Mean: PM_{10}: 0.11 ng m^{-3}	Gly > Asp > Ala	
Dome C station, Antarctic (3233m)	Polar (Aerosol)	12/2012-01/2013 (summer) PM_{10} and cascade impactor 5 samples		Mean: PM_{10}: 0.1 ng m^{-3}	Gly > Asp > Ala	
Rose Sea (Cruise)	Marine (Aerosol)	11-12/2011 TSP 5 samples		Mean: TSP: 0.48 ng m^{-3}	Gly > Pro = Glu	
Gruvebadet observatory, Svalbard, Artic (8 m)	Polar (Aerosol)	04-06/2015 Cascade impactor 7 samples	HPLC-MS/MS	Mean: 6.1 ± 3.4 pmol m^{-3} Mean Gly: 0.27 ng m^{-3} Range PM_{10}: 2.0-10.8 pmol m^{-3}	Gly > Ala > Asp	Feltracco et al. (2019)
Zeppelin observatory Svalbard, Arctic (420 m)	Polar (Aerosol)	09-12/2015 (winter) Coarse (2 - 10 µm) Fine (< 2 µm) 40 samples	HPLC (MS/MS) C_4-NA-NHS-Derivatization	Range TAA: Fine: 6 - 2914 pmol m^{-3} Coarse: 0.02 - 1417 pmol m^{-3}	Leu > Ala > Val	Mashayekhy Rad et al. (2019)

Lists of acronyms

- AQC: Molecular composition of the water-soluble fraction of atmospheric carbonaceous
- C_4-NA-NHS: N-butyl nicotinic acid Nhydroxysuccinimide ester
- DABS-Cl: 4-dimethylaminoazobenzene-40-sulfonyl chloride
- MTBSTFA: N-(t-butyldimethylsilyl)-N-methyltrifluoroacetamide
- OPA: ortho-phthalaldehyde
- tBDMS : Gly-tert-butyl dimethylsilyl
- TSP: Total suspended particles
- GC: Gas chromatography
- HPLC: high performance liquid chromatography
- IRMS: Isotope Ratio Mass Spectrometry

Estimated lifetimes of AAs : Description of the calculations performed in Table 4.

1- Calculations of the lifetimes considering theoretical $HO^•$, O_3 and $^1O_2^*$ concentrations (column (A) in Table 4)

Aqueous concentrations of $HO^•$, O_3 and $^1O_2^*$ are respectively equal to 10^{-14}, 5.0 10^{-10} and 1.0 10^{-12} M. The concentration of $HO^•$ derives from the study of Arakaki et al. (2013); the concentration of O_3 is calculated considering a 50 ppb concentration of gaseous O_3 and its Henry's law constant ($H(O_3) = 10^{-3}$ M atm^{-1}). $^1O_2^*$ concentration is estimated to be 2 orders of magnitude more concentrated than $HO^•$. All the kinetic constants derive from the Jaber et al. (2021) study (considering T and pH-dependency when necessary and available). The lifetimes for individual AA are calculated as following:

$$\tau = \frac{1}{k_{HO} \times [HO^{\cdot}] + k_{O_3} \times [O_3] + k_{^1O_2^*} \times [\,^1O_2^{\,*}]}$$

2- Calculations of the lifetimes using irradiation experiments in artificial cloud medium (column (D) in Table 4)

Experimental irradiation of 19 amino acids at a concentration of 1 µM each in an artificial cloud medium were conducted in Jaber et al. (2021). $HO^•$ production was performed using Fe-Ethylenediamine-N,N′-disuccinic acid (EDDS) complex solution. $HO^•$ concentration of 8.3 10^{-13} M was estimated during the experiment. Abiotic transformation rates ($R_{photo,exp}$) are evaluated during the experiment in mol L^{-1} h^{-1} (see Table 2 in Jaber et al., 2021). For Arg, Asn, Asp, Gln, Gly, Lys and Pro, lifetimes cannot be calculated since a production is observed during the experiment.

The lifetimes for individual AA are calculated as follows:

$$\tau = \frac{[AA]}{R_{photo,exp} \cdot \frac{[HO^{\cdot}]_{photo.exp}}{[HO^{\cdot}]_{cloud}}}$$

$[AA]$ represents the initial AA concentration in the experiment, *i.e.,* 1 µM.

Since the experiments were conducted with $HO^•$ concentrations likely higher than ambient ones in cloud water, we correct these abiotic rates to $HO^•$ concentrations in clouds by $[HO^{\cdot}]_{photo.exp}$ = 8.3 × 10^{-13} M and $[HO^{\cdot}]_{cloud}$ = 10^{-14} M. This correction has been considered as in Jaber et al. (2021) to fit the abiotic rates to an $HO^•$ concentration of 10^{-14}M.

3- Calculations of the lifetimes using biodegradation experiments in artificial cloud medium (column (F) in Table 4)

Biodegradation experiments of 19 amino acids were performed by Jaber et al. (2021) using 4 microbial strains (*Rhodococcus enclensis* PDD-23b-28, *Pseudomonas graminis* PDD-13b-3, *Pseudomonas syringae* PDD-32b-74 and *Sphingomonas sp.* PDD-32b-11) in artificial cloud water. Biodegradation rates are evaluated experimentally in mol cell^{-1} h^{-1} (see Table 1 in Jaber et al., 2021). These values are multiplied by 6.8 10^7 cells L^{-1} which corresponds to the average concentration of microorganisms in cloud water reported at PUY (Vaïtilingom et al., 2012). This leads to the values R_{23b-28}, R_{13b-3}, R_{32b-74}, R_{32b-11} in mol L^{-1} h^{-1}. *Rhodococcus enclensis* PDD-23b-28, *Pseudomonas graminis* PDD-13b-3, *Pseudomonas syringae* PDD-32b-74 and *Sphingomonas sp.* PDD-32b-11 contributes respectively to 6.3 %, 14.9 %, 14.9 % and 16.2% of the total cell concentration. The remaining 47.7 % belongs to other phyla or classes. We scale up each contribution by a factor 1.91 (=100/52.3), implying that the four bacteria types are representative for the remainder (47.7 %) of the bacteria population.

Therefore, we calculate the atmospheric lifetimes for individual AA as following:

$$\tau = \frac{[AA]}{0.063\,R_{23b-28} \cdot 1.91 - 0.149\,R_{13b-3} \cdot 1.91 - 0.149\,R_{32b-74} \cdot 1.91 - 0.162\,R_{32b-11} \cdot 1.91}$$

$[AA]$ represents the initial AA concentration in the experiment, *i.e.,* 1 µM.

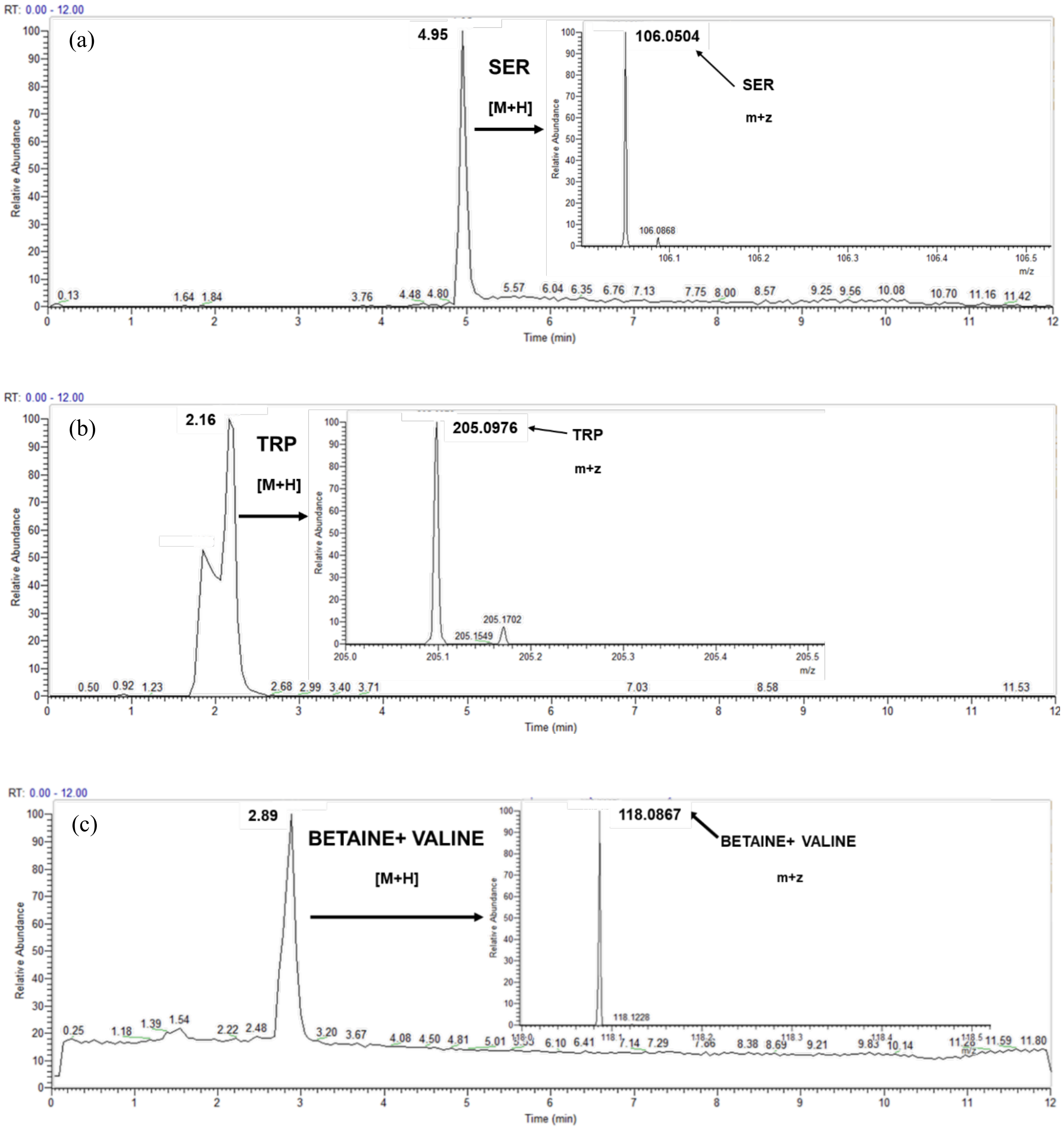

Figure S1. Chromatograms and MS spectra of: (a) Ser, (b) Trp and (c) Val (+ Betaine) measured by UPLC-HRMS (11-Mar-20 Cloud).

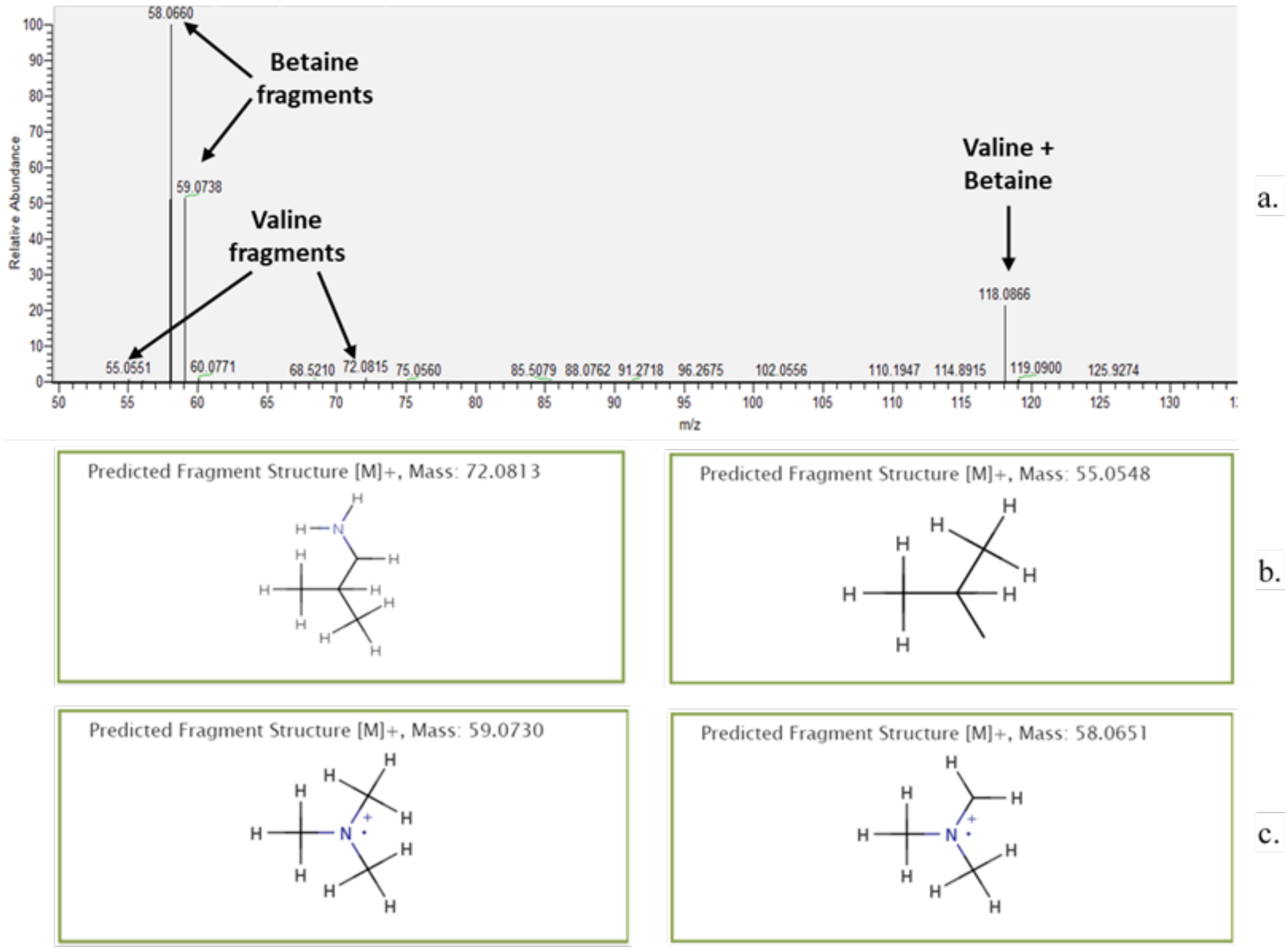

Figure S2. a. MS/MS of the compounds at m/z 118.0866 $[M+H]^+$ detected on 11-Mar cloud, and the characteristic product ions: b. Predicted structures and values of Betaine fragments m/z = 58.0651 and 59.0730 $[M+H]^+$; c. Predicted structures and values of Valine fragments m/z = 55.0548 and 72.0813 $[M+H]^+$. Predicted values and structures are issued from MetLIN Mass Spectral Database.

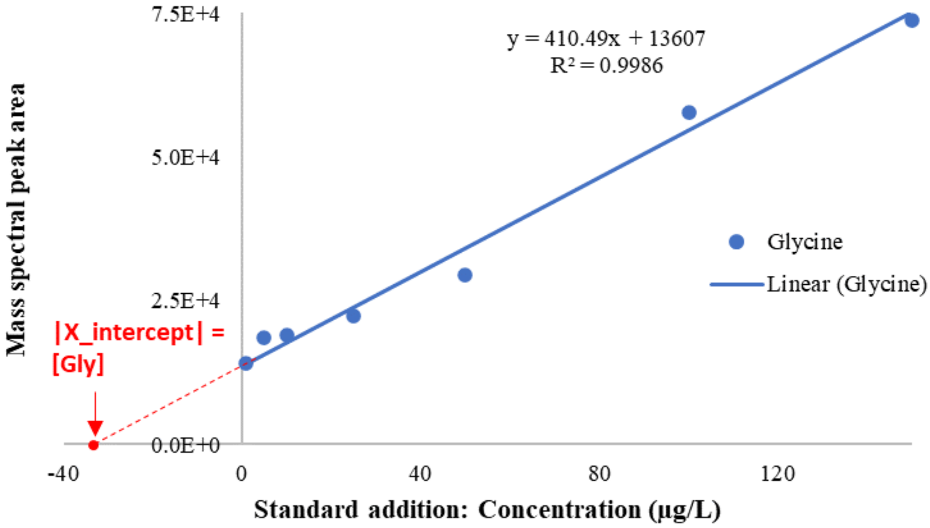

Figure S3. Quantification of amino acid concentrations (11-Mar-20 cloud sample) using the addition standard method: case study of glycine (Gly).

Quantification and uncertainty (Figure S3): STD$_M$

In standard addition, known quantities of analyte (AA) are added to the unknown quantity in the sample. From the increase in signal, we deduce how much analyte was originally in the sample. This method requires a linear response to analyte (Broekaert, 2015).

The magnitude of the intercept on the x-axis is the original concentration of Gly. The equation of the trendline is y = a x + b. The x_intercept is obtained by setting y = 0: x = -b / a, with a = slope of the curve, b = y_intercept, x = the concentration of the AA, y= the mass spectral area:

Gly: a = 410.49; b = 13607 → |x_intercept| = [Gly] = 33.1 µg L^{-1} (negative value)

The obtained values are then corrected by the dilution factor of 10 % (due to the ratio 9:1 volume cloud: volume added standard). Final value is: [Gly]= 33.1 × $\frac{10}{9}$ = 36.8 µg L^{-1}.

The uncertainty in the x_intercept is s_x:

$$s_x = \frac{s_y}{|a|}\sqrt{\frac{1}{n} + \frac{\bar{y}^2}{a^2 \times \sum(x_i - \bar{x})^2}}$$

where a is the absolute value of the slope of the trendline, n is the number of data points, $\bar{y}$ is the mean value of y for the points, x_i are the individual values of x, $\bar{x}$ is the mean value of y for the points, and s_y is the standard deviation for y:

$$\mathrm{STD_M} = s_y = \sqrt{\frac{1}{(n-2)} \times \left[\sum((y-\bar{y})^2 - \frac{[\sum(x-\bar{x})(y-\bar{y})]^2}{\sum(x-\bar{x})^2}\right]}$$

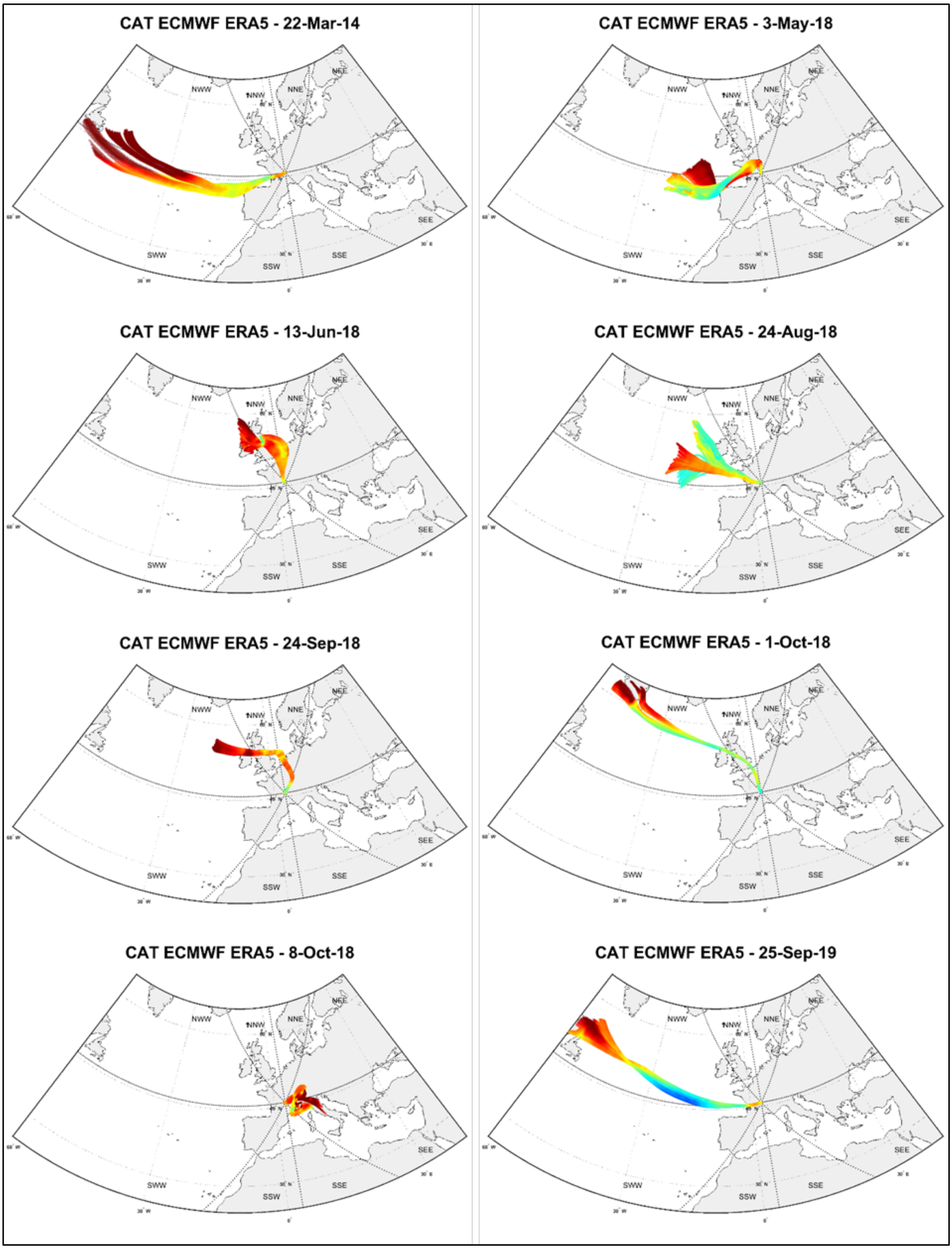
CAT ECMWF ERA5 - 22-Mar-14
NWW
NNW
NNE
NEE
SEE
SWW
SSW
SSE
CAT ECMWF ERA5 - 3-May-18
NWW
NNW
NNE
NEE
SEE
SWW
SSW
SSE
CAT ECMWF ERA5 - 13-Jun-18
NWW
NNW
NNE
NEE
SEE
SWW
SSW
SSE
CAT ECMWF ERA5 - 24-Aug-18
NWW
NNW
NNE
NEE
SEE
SWW
SSW
SSE
CAT ECMWF ERA5 - 24-Sep-18
NWW
NNW
NNE
NEE
SEE
SWW
SSW
SSE
CAT ECMWF ERA5 - 1-Oct-18
NWW
NNW
NNE
NEE
SEE
SWW
SSW
SSE
CAT ECMWF ERA5 - 8-Oct-18
NWW
NNW
NNE
NEE
SEE
SWW
SSW
SSE
CAT ECMWF ERA5 - 25-Sep-19
NWW
NNW
NNE
NEE
SEE
SWW
SSW
SSE

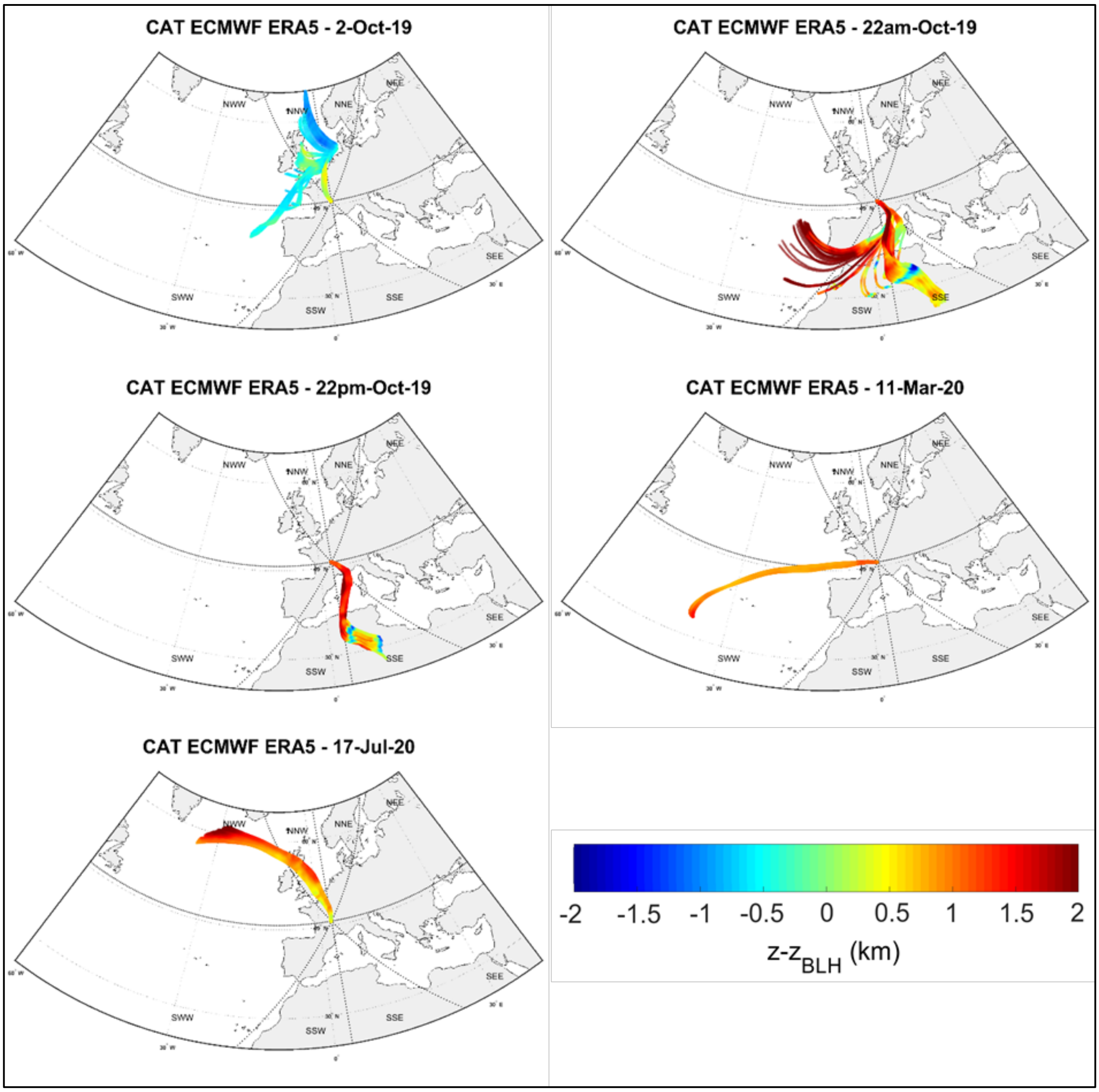

Figure S4. Individual CAT model back trajectories of each of the 13 cloud events reaching PUY. Colors correspond to the air mass height minus the atmospheric boundary layer height (ABLH). Positive values (> ABLH, red) indicate the air mass is in the free troposphere. Negative values (< ABLH, blue) indicate the air mass is in the boundary layer. ABLH is the boundary layer height parameter of the ECMWF ERA5 (European Centre for Medium-Range Weather Forecasts Reanalysis v5). Its calculation is based on the bulk Richardson number following the conclusions of Seidel et al. (2012). A more detailed description of this parameter and its calculation can be found in the ECMWF operational implementation document (available at: https://confluence.ecmwf.int/display/CKB/ERA5).

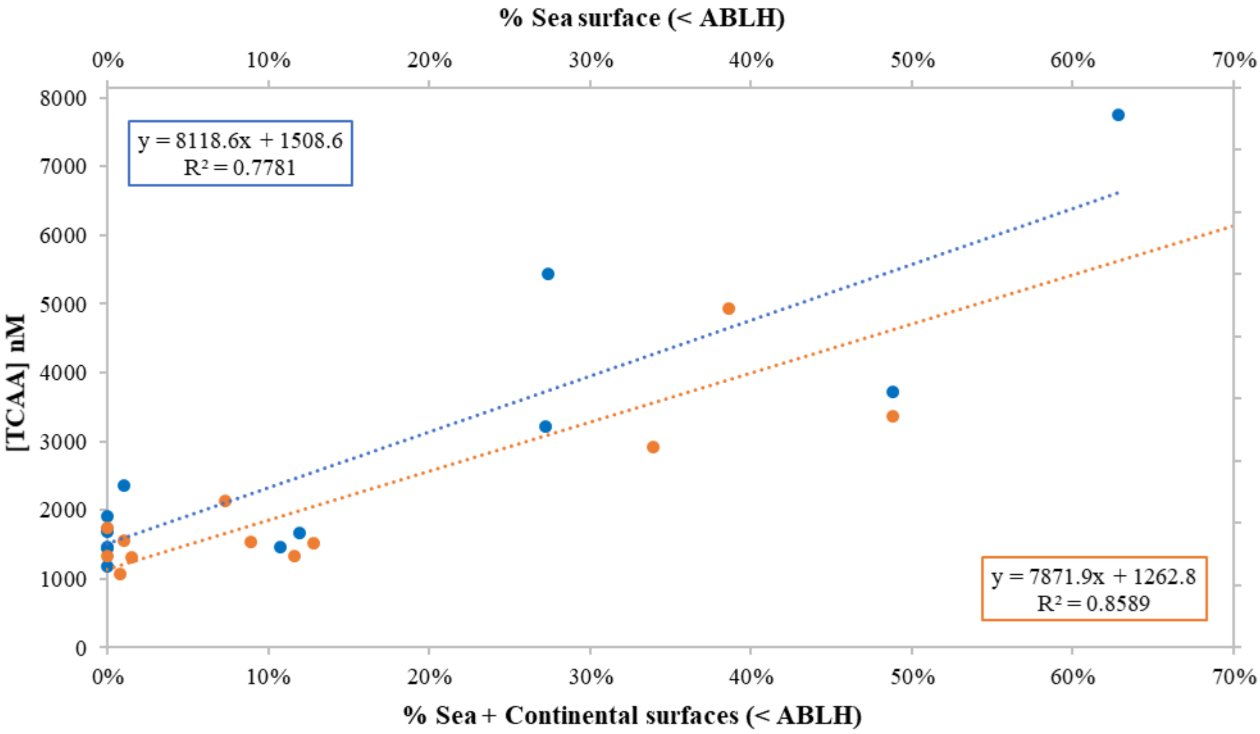

Figure S5. Correlation between total concentration of 18 AAs (TCAA) and the percentage of time spent above: in blue, the Sea surface (< ABLH); and in orange, the Sea plus the Continental surfaces (< ABLH).

References

Barbaro, E., Morabito, E., Gregoris, E., Feltracco, M., Gabrieli, J., Vardè, M., Cairns, W.R.L., Dallo, F., De Blasi, F., Zangrando, R., Barbante, C., Gambaro, A.: Col Margherita Observatory: A background site in the Eastern Italian Alps for investigating the chemical composition of atmospheric aerosols, Atmos. Environ., 221, 117071, 2020.

Barbaro, E., Zangrando, R., Moret, I., Barbante, C., Cescon, P., Gambaro, A.: Free amino acids in atmospheric particulate matter of Venice, Italy, Atmos. Environ., 45, 5050-5057, 2011.

Barbaro, E., Zangrando, R., Vecchiato, M., Piazza, R., Cairns, W.R.L., Capodaglio, G., Barbante, C., Gambaro, A.: Free amino acids in Antarctic aerosol: potential markers for the evolution and fate of marine aerosol, Atmos. Chem. Phys., 15, 5457-5469, 2015.

Bianco, A., Voyard, G., Deguillaume, L., Mailhot, G., Brigante, M.: Improving the characterization of dissolved organic carbon in cloud water: Amino acids and their impact on the oxidant capacity, Sci. Rep., 6, 37420, 2016.

Broekaert, J.A.C.: Daniel C. Harris: Quantitative chemical analysis, 9th ed, Analytical and Bioanalytical Chem., 407, 8943-8944, 2015.

Di Filippo, P., Pomata, D., Riccardi, C., Buiarelli, F., Gallo, V., Quaranta, A.: Free and combined amino acids in size-segregated atmospheric aerosol samples, Atmos. Environ., 98, 179-189, 2014.

Feltracco, M., Barbaro, E., Kirchgeorg, T., Spolaor, A., Turetta, C., Zangrando, R., Barbante, C., Gambaro, A.: Free and combined L- and D-amino acids in Arctic aerosol, Chemosphere, 220, 412-421, 2019.

Helin, A., Sietiö, O.M., Heinonsalo, J., Bäck, J., Riekkola, M.L., Parshintsev, J.: Characterization of free amino acids, bacteria and fungi in size-segregated atmospheric aerosols in boreal forest: seasonal patterns, abundances and size distributions, Atmos. Chem. Phys., 17, 13089-13101, 2017.

Mace, K.A., Kubilay, N., Duce, R.A.: Organic nitrogen in rain and aerosol in the eastern Mediterranean atmosphere: An association with atmospheric dust, J. Geophys. Res.: Atmospheres, 108, 2003a.

Mace, K.A., Duce, R.A., Tindale, N.W.: Organic nitrogen in rain and aerosol at Cape Grim, Tasmania, Australia, J. Geophys. Res.: Atmospheres, 108, 2003b.

Mandalakis, M., Apostolaki, M., Tziaras, T., Polymenakou, P., Stephanou, E.G.: Free and combined amino acids in marine background atmospheric aerosols over the Eastern Mediterranean, Atmos. Environ., 45, 1003-1009, 2011.

Mashayekhy Rad, F., Zurita, J., Gilles, P., Rutgeerts, L.A.J., Nilsson, U., Ilag, L.L., Leck, C.: Measurements of atmospheric proteinaceous aerosol in the Arctic using a selective UHPLC/ESI-MS/MS strategy, Journal of The American Society for Mass Spectrometry, 30, 161-173, 2019.

Matsumoto, K., Uematsu, M.: Free amino acids in marine aerosols over the western North Pacific Ocean, Atmos. Environ., 39, 2163-2170, 2005.

Mopper, K., Zika, R.G.: Free amino acids in marine rains: evidence for oxidation and potential role in nitrogen cycling, Nature, 325, 246-249, 1987.

Ren, L., Bai, H., Yu, X., Wu, F., Yue, S., Ren, H., Li, L., Lai, S., Sun, Y., Wang, Z., Fu, P.: Molecular composition and seasonal variation of amino acids in urban aerosols from Beijing, China, Atmos. Res., 203, 28-35, 2018.

Ruiz-Jimenez, J., Okuljar, M., Sietiö, O.M., Demaria, G., Liangsupree, T., Zagatti, E., Aalto, J., Hartonen, K., Heinonsalo, J., Bäck, J., Petäjä, T., Riekkola, M.L.: Determination of free amino acids, saccharides, and selected microbes in biogenic atmospheric aerosols – seasonal variations, particle size distribution, chemical and microbial relations, Atmos. Chem. Phys., 21, 8775-8790, 2021.

Samy, S., Robinson, J., Hays, M.D.: An advanced LC-MS (Q-TOF) technique for the detection of amino acids in atmospheric aerosols, Analytical and Bioanalytical Chem., 401, 3103-3113, 2011.

Samy, S., Robinson, J., Rumsey, I.C., Walker, J.T., Hays, M.D.: Speciation and trends of organic nitrogen in southeastern U.S. fine particulate matter (PM2.5), J. Geophys. Res.: Atmospheres, 118, 1996-2006, 2013.

Scalabrin, E., Zangrando, R., Barbaro, E., Kehrwald, N.M., Gabrieli, J., Barbante, C., Gambaro, A.: Amino acids in Arctic aerosols, Atmos. Chem. Phys., 12, 10453-10463, 2012.

Seidel, D., Zhang, Y., Beljaars, A., Golaz, J.-C., Medeiros, B.: Climatology of the planetary boundary layer over continental United States and Europe, J. Geophys. Res., 117, D17106, 2012.

Song, T., Wang, S., Zhang, Y., Song, J., Liu, F., Fu, P., Shiraiwa, M., Xie, Z., Yue, D., Zhong, L., Zheng, J., Lai, S.: Proteins and amino acids in fine particulate matter in rural Guangzhou, Southern China: seasonal cycles, sources, and atmospheric processes, Environ. Sci. & Technol., 51, 6773-6781, 2017.

Triesch, N., van Pinxteren, M., Engel, A., Herrmann, H.: Concerted measurements of free amino acids at the Cape Verde Islands: High enrichments in submicron sea spray aerosol particles and cloud droplets, Atmos. Chem. Phys., 21, 163-181, 2021.

Violaki, K., Mihalopoulos, N.: Water-soluble organic nitrogen (WSON) in size-segregated atmospheric particles over the Eastern Mediterranean, Atmos. Environ., 44, 4339-4345, 2010.

Wedyan, M.A., Preston, M.R.: The coupling of surface seawater organic nitrogen and the marine aerosol as inferred from enantiomer-specific amino acid analysis, Atmos. Environ., 42, 8698-8705, 2008.

Xu, Y., Wu, D., Xiao, H., Zhou, J.: Dissolved hydrolyzed amino acids in precipitation in suburban Guiyang, southwestern China: Seasonal variations and potential atmospheric processes, Atmos. Environ., 211, 247-255, 2019.

Yan, G., Kim, G., Kim, J., Jeong, Y.-S., Kim, Y.I.: Dissolved total hydrolyzable enantiomeric amino acids in precipitation: Implications on bacterial contributions to atmospheric organic matter, Geochimica et Cosmochimica Acta, 153, 1-14, 2015.

Yang, H., Xu, J., Wu, W.-S., Wan, C.H., Yu, J.Z.: Chemical characterization of water-soluble organic aerosols at Jeju Island collected during ACE-Asia, Environ. Chem., 1, 13-17, 2004.

Yang, H., Yu, J.Z., Ho, S.S.H., Xu, J., Wu, W.-S., Wan, C.H., et al.: The chemical composition of inorganic and carbonaceous materials in PM2.5 in Nanjing, China, Atmos. Environ., 39, 3735-3749, 2005.

Zhang, Q., Anastasio, C.: Free and combined amino compounds in atmospheric fine particles (PM2.5) and fog waters from Northern California, Atmos. Environ., 37, 2247-2258, 2003.

Zhu, R.G., Xiao, H.Y., Luo, L., Xiao, H., Wen, Z., Zhu, Y., Fang, X., Pan, Y., Chen, Z.: Measurement report: Hydrolyzed amino acids in fine and coarse atmospheric aerosol in Nanchang, China: concentrations, compositions, sources and possible bacterial degradation state, Atmos. Chem. Phys., 21, 2585-2600, 2021.